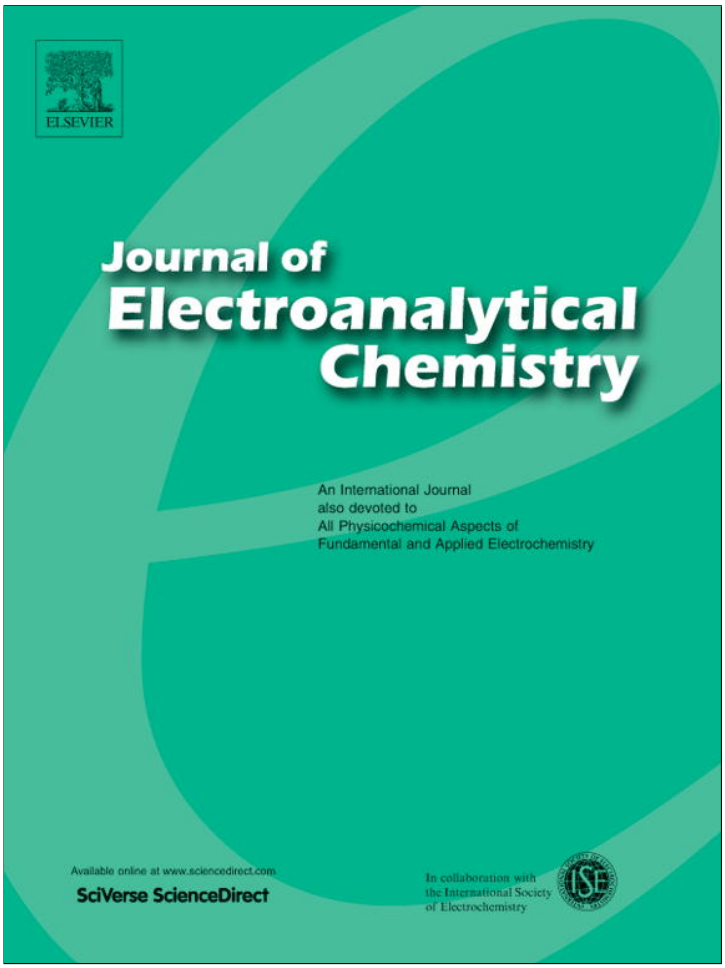

(This is a sample cover image for this issue. The actual cover is not yet available at this time.)

Journal of Electroanalytical Chemistry 691 (2013) 42–50

Contents lists available at SciVerse ScienceDirect

Journal of Electroanalytical Chemistry

journal homepage: www.elsevier.com/locate/jelechem

Nucleation and growth of silver nanostructures onto HOPG electrodes in the presence of picolinic acid

Cecilia I. Vázquez, Gabriela I. Lacconi *

INFIQC, Departamento de Fisicoquímica, Facultad de Ciencias Químicas, Universidad Nacional de Córdoba, Haya de la Torre – Medina Allende, Ciudad Universitaria, 5000 Córdoba, Argentina

ARTICLE INFO

Article history:
Received 6 October 2012
Received in revised form 17 December 2012
Accepted 21 December 2012
Available online 4 January 2013

Keywords:
Silver nanostructures
Nucleation and growth
Electrocrystallization
Picolinic acid

ABSTRACT

Silver electrodeposition onto HOPG electrodes in the presence of picolinic acid (PA) has been studied by cyclic voltammetry and chronoamperometry. Changes in the nucleation and growth mechanisms, which are dependent on the PA concentration and solution pH, have been observed. Formation of complexes with Ag^+ ions and adsorption of the additive molecules on both, the substrate and the growing silver crystallites can be correlated with the potential dependence of the kinetic parameters, N_0 and A. The amount, distribution (random or localized on the defects sites) and size of the crystallites on the substrate are influenced by the composition of the solution (PA concentration and pH) when the control of the nucleation and growth processes is regulated by application of a double potential program.

1. Introduction

For many years, use of electrodeposition methods in metal coating research has intensified with growing technological interest to acquire a better understanding of the role played by the additives in the global process. At a macroscopic level, it is well known that the organic additives fulfill functions as leveling and brightening agents [1–3]. Organic molecules containing functional groups have a strong influence on the kinetics of the first stages of the electrocrystallization process, thereby promoting the formation of metallic films with different properties and morphology [4–6]. Despite the diversity of studies conducted in this area, only limited amounts of information about the activity of additives during electroformation of nanodimensional metal structures are currently available. When the dimension of the deposited metal structures approaches the nanometer range, the initial stages of electrocrystallization, i.e. the nucleation and growth, become very important [7–9]. Nuclei formation can be regarded as the most critical stage in the process mechanism for establishing the final particle properties [9,10].

Silver nucleation mechanisms on different electrodes from various electrolytes have been extensively studied [10–15]. The surface state of the substrate, and the temperature and composition of the electrolyte play an important role in the mechanism of silver nanoparticles deposition. Most research has shown that silver deposition in additive-free electrolytes occurs by an instantaneous nucleation mechanism [16–18], whereas the mechanism of silver growth on substrates such as crystalline silicon or highly oriented pyrolitic graphite (HOPG) corresponds to the Volmer–Weber growth, which is very important to induce only the formation of 3D crystallites [10,19]. When the electrolyte contains small amounts of organic compounds, changes on the characteristics of the deposited particles (homogeneity distribution, shape, size, and number density) are observed. The resulting morphology of the crystallites is generally related to the adsorption of the additive molecules on the electrode or on the growing clusters, and the additive adsorption process has been shown to have an important influence on the electron transfer kinetics and, consequently, on the nucleation of the metallic clusters [20].

Picolinic acid (PA) is an organic compound with chemical structure simple, inexpensive and easy to obtain, however there are currently very few publications concerning to the use of pyridine–carboxylic acids, as additives in plating process. For example, PA was demonstrated to be an efficient leveler agent in copper electrodeposition, mainly for its tendency to form complexes with metallic ions and its adsorption capacity on various surfaces, via their functional groups [21,22]. In the present study, we have used PA as an additive to establish its influence on the initial stages of Ag crystallites electrodeposition onto HOPG surfaces.

The aim of this work is to provide a better understanding of the underlying mechanisms of silver electrodeposition on HOPG electrodes on the basis of electrochemical results from cyclic voltammetry and chronoamperometry in the presence of picolinic acid (PA). The influence of different acid–base species of the additive, and the corresponding complexes with Ag^+ ions in solution, on the nucleation and growth kinetics of silver nanostructures is discussed in detail.

* Corresponding author. Tel.: +54 351 4334169; fax: +54 351 4334188.
E-mail addresses: glacconi@mail.fcq.unc.edu.ar, Gabriela.Lacconi@gmail.com (G.I. Lacconi).

1572-6657/$ - see front matter © 2012 Elsevier B.V. All rights reserved.
http://dx.doi.org/10.1016/j.jelechem.2012.12.017

2. Experimental

All solutions were prepared from analytical grade reagents and purified water by a Millipore Milli-Q system. The electrolyte employed was 1 mM $AgClO_4$ (BDH Chemicals Ltd.) in 0.5 M $HClO_4$ (J.T. Baker) at pH 0.3, or in 0.1 M $KClO_4$ at pH 3.0 and 6.5. Picolinic acid (Sigma–Aldrich) was added to the electrolyte, and solutions with concentrations ranging from 0.5 to 5.0 mM were prepared. The pH of the electrolyte was adjusted by addition of $HClO_4$ or KOH concentrated solutions. The aqueous solutions were freshly prepared and saturated with purified nitrogen before every experiment.

Analytical determinations of the species in solution were carried out by Nuclear Magnetic Resonance spectroscopy (NMR) with a BRUKER 400 MHz spectrometer (Advance II) containing a BBI inverse detection probe. The ^{1}H NMR spectra were recorded for 5.0 mM PA solutions, after addition of different amounts of $AgClO_4$ at pH 3.0 and 6.5 (10% deuterated water) with a constant ionic strength of 0.1 M. Benzene was added as an internal standard.

Electrochemical measurements were carried out in a conventional three-electrode glass cell system at room temperature. HOPG plates (SPI Supplies, Brand Grade SPI-1, 10×10 mm^2), previously cleaved with adhesive tape and introduced in a Teflon holder were used as working electrodes. A platinum foil and a silver wire directly immersed in the electrolyte were used as counter and quasi-reference electrodes, respectively. All potentials are reported vs. Ag°/Ag^+ (1.0 mM) reference electrode ($E_{Ag^\circ/Ag+} = -0.30$ V vs. SCE).

Potentiodynamic experiments were recorded at a scan rate of 0.02 V s^{-1} in the potential range from +0.5 to −0.4 V with a computer-controlled potentiostat Autolab PGSTAT with GPES software (ECO CHEMIE B.V.). Prior to each electrochemical experiment, a reproducible state of the HOPG surface was produced by polarization of the electrode at 0.4 V for about 3 min in the electrolyte [23]. Application of this conditioning pretreatment is necessary due to the initial presence of a cathodic current given by the intrinsic nucleation sites on the freshly cleaved graphite surface at open circuit potential [24]. The deposition of silver crystallites was carried out under potentiostatic conditions by application of either a single or double potential step. All current densities were normalized in terms of the apparent geometric area of the HOPG electrode.

The morphology of Ag crystallites was examined using a scanning electron microscopy (SEM) JEOL JSM-7401F Field Emission Gun Scanning Electron Microscope (FEG-SEM), with data acquired in the LEI mode, with a gun tension of 5 kV.

3. Results and discussion

3.1. Composition of the PA electrolyte

Picolinic acid has two acidic functions with thermodynamic dissociation constants of $pK_1 = 1.03$ and $pK_2 = 5.21$ [25], corresponding to the dissociation of the carboxyl group and the protonated ring nitrogen, respectively. Reaction scheme (1) shows the different acid–base species of PA, labeled as ***H_2Pic^+*** (protonated), ***HPic*** (zwitterion) and ***Pic^-*** (anion).

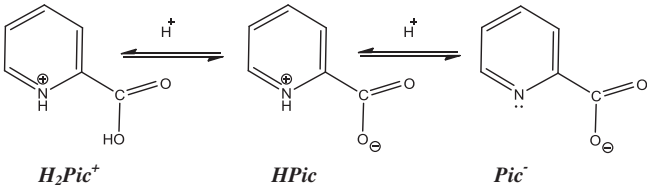

(1)

It is noteworthy that depending on the solution pH, the PA species in solution can form soluble complexes with the Ag^+ ions. For example, the relevant PA chemical species in solution are the protonated ***H_2Pic^+*** at pH 0.3, the zwitterion ***HPic*** at pH 3.0 and the anion ***Pic^-*** at pH 6.5. It is important to notice that the concentration of [***Ag***(***L***)$^+$] complexes in solution, with ***HPic*** and ***Pic^-*** species as ligands, can be regulated by changing the pH. In the present case, the formation of complexes with the protonated species ***H_2Pic^+*** is not considered because it has not available functional groups.

In order to study the silver electrodeposition mechanism in the presence of PA, knowledge of the stability constants for the silver complexes with the different PA species was required. In this work, the formation constants were determined by analysis of solution nuclear magnetic resonance (NMR) spectra. The chemical shifts from ^{1}H NMR spectra provide an estimate for the degree of electronic perturbation of the ligand species caused by the Ag^+ ions, thereby allowing the chemical structures and stability constants of silver complexes to be determined [26–29].

The comparative analysis of the spectra (results not shown) of 5 mM PA solutions supported the following statements regarding the complexes' chemical structure:

- The [***Ag***(***HPic***)$^+$] and [***Ag***(***Pic***)] species at pH 3.0 and 6.5, respectively, are formed by the interaction between Ag^+ ions and the carboxylate group of the PA species.
- Evidence of silver complexes formation was obtained by monitoring the changes in the chemical shifts (around 0.2 ppm) when titration of PA ligands (at every pH), with Ag^+ ions is performed [28,29].
- The values of calculated constants in concentrations (*Kc*) for [***Ag***(***L***)$^+$] complexes with 1:1 stoichiometry are given by reactions (2) and (3).

$$\boldsymbol{Ag}^+ + \boldsymbol{HPic} \rightleftarrows [\boldsymbol{Ag}(\boldsymbol{HPic})^+] \quad K_{1:1}(\text{pH } 3.0) = (11.5 \pm 0.6)\ \text{M}^{-1} \tag{2}$$

$$\boldsymbol{Ag}^+ + \boldsymbol{Pic}^- \rightleftarrows [\boldsymbol{Ag}(\boldsymbol{Pic})] \quad K_{1:1}(\text{pH } 6.5) = (800 \pm 100)\ \text{M}^{-1} \tag{3}$$

From the complexation constants, the chemical composition of the electrolytes at three pH values can be established.

3.2. Potentiodynamic deposition of silver from PA containing solutions

In order to establish the potential region for silver deposition onto HOPG electrodes, the voltammetric behavior in aqueous solutions containing PA was analyzed. The potentiodynamic profiles of HOPG in 1.0 mM $AgClO_4$ aqueous solutions in the absence (red curves) and presence (black curves) of 0.5 mM PA at pH 0.3 (a), 3.0 (b) and 6.5 (c), are shown in Fig. 1. The comparison between the *j*/*E* potentiodynamic profiles recorded in the absence of additive shows similar behavior, irrespective of the solution pH. There is one well-defined current peak for silver electrodeposition and the corresponding anodic peak, due to the silver dissolution process. The cathodic peak at around −0.23 V corresponds to the electroreduction of silver ions on the HOPG, according to the reaction:

$$Ag^+ + 1e \rightarrow Ag^\circ \tag{4}$$

Regardless of the pH, the potential of the cathodic and anodic peaks does not change with the pH. It is due to the same process is occurring in all solutions. However, the charge involved in the whole voltammogram (mainly in the dissolution process) diminishes notably as the pH is increased [30]. Furthermore, evidence of the process irreversibility is shown by the anodic peak shifting to more positive potentials, a feature that some authors have related to the silver oxidation with the formation of Ag(OH) species or silver oxide complexes with perchlorate ions [30–32].

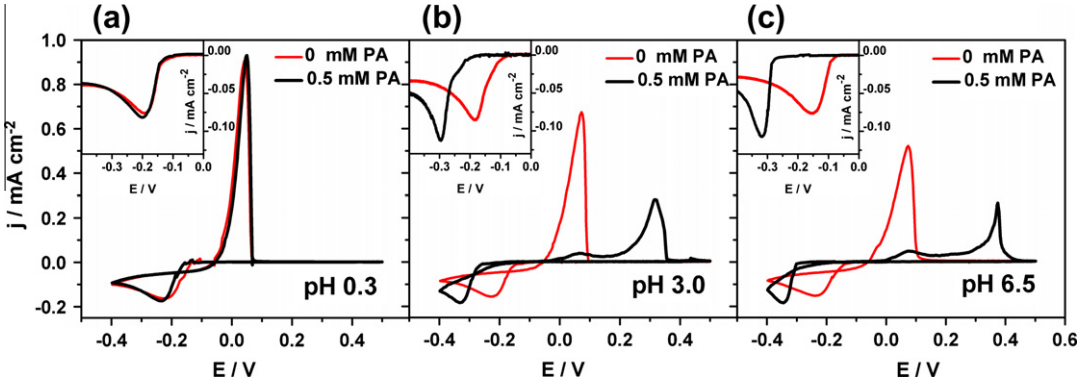

Fig. 1. Potentiodynamic j/E profiles of HOPG electrodes in 0.5 M $HClO_4$ (pH 0.3) or 0.1 M $KClO_4$ (pH 3.0 and 6.5) + 1.0 mM $AgClO_4$ + x mM PA (x = 0 (red curves), x = 0.5 (black curves)) at pH of 0.3 (a); 3.0 (b) and 6.5 (c). Scan rate: 0.02 V s^{-1}. Inset: negative potential scan at 0.005 V s^{-1}. (For interpretation of the references to colour in this figure legend, the reader is referred to the web version of this article.)

Fig. 1 also shows the j/E potentiodynamic profiles for silver deposition in the presence of 0.5 mM PA at different pH. At pH 0.3, both voltammograms (in the absence and presence of PA) are similar, with the cathodic and anodic peaks practically unchanged (Fig. 1a). Only a slight shifting of the onset potential for silver deposition towards negative values is observed (black curve), which is associated with adsorption of the additive. The potentiodynamic results indicate that, at this pH, addition of PA to the electrolyte has not a significant effect on silver electrocrystallization onto HOPG electrodes.

The potentiodynamic profiles recorded in solutions containing 0.5 mM PA at pH 3.0 and 6.5 are shown in Fig. 1b and c, respectively. In solutions of pH 3.0 the onset potential for nucleation and growth of silver clusters is around −0.28 V, in the presence of additive. Furthermore, by increasing the pH and PA content (results not shown), a progressive shifting in the cathodic peak potential is observed. In fact, the presence of PA can decrease the rate of deposition on the basis that the additive molecules can be adsorbed on the surface, blocking some nucleation sites or forming complexes in the solution [21,33]. At a pH of 6.5, formation of [***Ag***(***Pic***)] complexes is favored by the stability constant (reaction (3)) and silver deposition could be resulting from their electroreduction. In the case of silver deposition at pH 3.0, the cathodic peak potential is the same as that at pH 6.5 and could be also related to electroreduction of the [***Ag***(***L***)$^+$] complexes. Considering the low value of the equilibrium constant of complexation (reaction (2)) with the ***HPic***, it is likely that at pH 3.0, the complexes [***Ag***(***L***)$^+$] corresponds to [***Ag***(***Pic***)]. This feature could be associated to a change of the surface pH on the electrode, and the acid–base equilibrium of PA in solution is modified. Further evidence for determining the chemical nature of the adsorbed complexes on the growing crystals can be established by in situ SERS (Surface Enhancement of Raman Spectroscopy) measurements, results that will be included in a forthcoming publication [29].

In addition, in the inset (Fig. 1b) a current shoulder at ca. −0.25 V is noticed at low scan rates at pH 3.0, which can be associated with the electroreduction of Ag^+ ions (reaction (4)) as it occurs at the same potential as silver deposition in the absence of additive. Under these conditions, the current intensity of the prepeak depends on the free-Ag^+ ions concentration in solution and electrocrystallization can be favored to occur at defect sites on the HOPG surface. Regarding this issue, it is well known that preferential nucleation of silver clusters on the HOPG step edges occurs at low overpotentials [34,35].

The reverse scan in the presence of PA (3.0 < pH < 6.5) shows two anodic current peaks for the stripping of silver crystallites. The less anodic peak occurs at around the same potential as in the free-additive solution (ca. 0.06 V), while the potential of the second peak depends on the pH and the PA content in the solution. These results can be explained if we consider that just as silver stripping begins, an insoluble film of Ag–PA complexes is formed on the Ag crystallites, leading to surface passivation, as well as other authors have shown in the presence of thiosulphate ions [36]. Consequently, a higher potential is necessary to achieve the dissolution of silver crystallites (anodic peak at around 0.35 V).

3.3. Current transients for silver deposition from PA containing solutions

In order to study the kinetics of silver nucleation onto HOPG electrodes in the presence of different chemical species of PA, a program of single potential pulse was applied. The potential was stepped from 0.4 V (see Section 2) to the silver electrodeposition potentials, established from the potentiodynamic experiments. Figs. 2a and 3a show a series of current transients for silver deposition at different potentials, recorded at pH 0.3, 3.0 and 6.5, in the absence and presence of PA, respectively. All current transients exhibit the typical shape for nucleation with a three-dimensional growth process, limited by diffusion of the electroactive species [13,37]. At short times, the current density maximum (denominated j_{max}) at t_{max} is due to the nucleation and growth of the new phase. At longer times, the current decays to reach a stationary value, and the process is controlled by mass transfer of the electroactive species towards the electrode surface.

The theoretical model of Sharifker and Hills for three-dimensional nucleation mechanism considers that the nuclei formed on the surface contribute to the overall surface area through individual diffusion zones, which regulate the supply of reactants from the bulk to the solution [38]. When local diffusion zones overlap, covering the electrode surface (maximum in the transient), the reaction approaches a steady state and the current decays as given by the Cottrell equation [39]. Depending on the growth rate, two limiting mechanisms for nucleation are established: instantaneous and progressive [34]. Non-dimensional plots $(j/j_{max})^2$ vs. time t/t_{max}, with the maxima coordinates from the current transients, were compared with the theoretical curves for the determination of the nucleation and growth mechanism (Figs. 2b and 3b). The theoretical curves correspond to the limiting cases given by Eqs. (5) and (6), for instantaneous (red curves) and progressive (green curves) nucleation, respectively [38].

Instantaneous Nucleation:

$$\left(\frac{j}{j_{max}}\right)^2 = 1.9542\left(\frac{t}{t_{max}}\right)\left[1-\exp\left(-1.2564\frac{t}{t_{max}}\right)\right]^2 \quad (5)$$

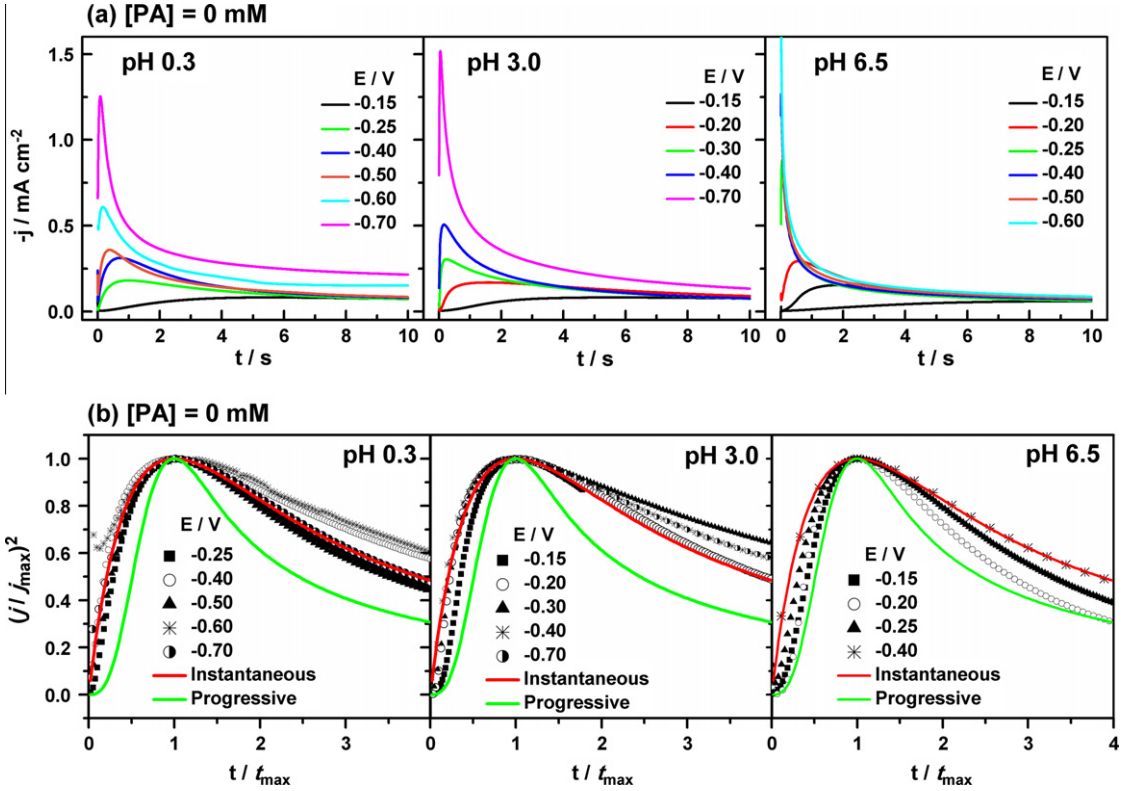

Fig. 2. (a) Current density transients for silver nucleation on HOPG electrodes at different potentials, in 0.5 M $HClO_4$ (pH 0.3) or 0.1 M $KClO_4$ (pH 3.0 and 6.5) + 1 mM $AgClO_4$; and (b) non-dimensional plots from data in (a). Theoretical curves for instantaneous (red curves) and progressive (green curves) nucleation. (For interpretation of the references to colour in this figure legend, the reader is referred to the web version of this article.)

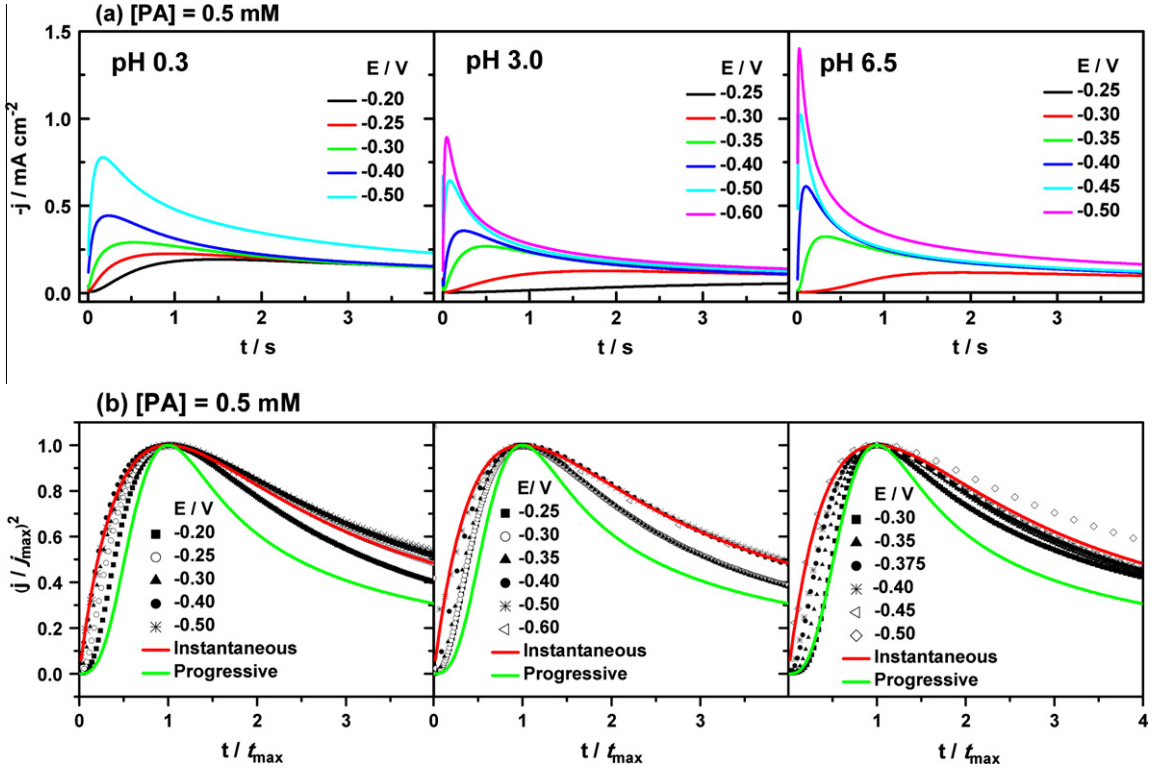

Fig. 3. (a) Current density transients for silver nucleation on HOPG electrodes at different potentials, in 0.5 M $HClO_4$ (pH 0.3) or 0.1 M $KClO_4$ (pH 3.0 and 6.5) + 1 mM $AgClO_4$ + 0.5 mM PA; (b) non-dimensional plots from data in (a). Theoretical curves for instantaneous (red curves) and progressive (green curves) nucleation. (For interpretation of the references to colour in this figure legend, the reader is referred to the web version of this article.)

and *Progressive Nucleation*:

$$\left(\frac{j}{j_{max}}\right)^2 = 1.2254\left(\frac{t}{t_{max}}\right)\left[1-\exp\left(-1.2564\frac{t^2}{t_{max}}\right)\right]^2 \quad (6)$$

Current transients for silver deposition onto HOPG electrodes at various potentials in solutions of 1.0 mM $AgClO_4$, at pH of 0.3, 3.0 and 6.5 in the absence of PA show convergence of the current curves to a stationary value, except for those at potentials more negative than −0.6 V (Fig. 2). This effect is more noticeable at low pH, where the extra contribution to the current is due to hydrogen evolution on the silver crystallites. The corresponding non-dimensional plots in the free-additive electrolyte (at pH 0.3 and 3.0), show that silver nuclei are formed just after applying the potential pulse, irrespective of the deposition potential. These results are in agreement with the 3D-instantaneous nucleation controlled by diffusion of Ag^+ ions, indicated by other authors [40]. However, at pH 6.5, there is a slight tendency towards a change from intermediate to instantaneous nucleation as the deposition potential becomes more negative. Thus, when we compare transients at the same deposition potential (−0.4 V) in the absence of additive, silver nucleation seems to be favored in solutions with higher pH (increase of j_{max}). As discussed below, a similar effect on the electrodeposition transients, when the solution contains PA, was also observed. The diffusion coefficients D for the Ag^+ ions calculated by linearization of the current decaying part at −0.4 V, according to the Cottrell equation were $D^{0.3} = 2.0 \times 10^{-5}$ cm^2 s^{-1}, $D^{3.0} = 1.9 \times 10^{-5}$ cm^2 s^{-1} and $D^{6.5} = 1.6 \times 10^{-5}$ cm^2 s^{-1} for pH 0.3, 3.0 and 6.5, respectively. These values are in good agreement with those reported in the literature [7,41].

Fig. 3a shows the series of current transients for silver deposition onto HOPG in solutions of 1.0 mM $AgClO_4$ + 0.5 mM PA at pH 0.3, 3.0 and 6.5. Similar to those observed in the absence of additive, the current transients at different potentials show the characteristic maximum from nucleation and crystal growth, followed by a decaying current corresponding to the planar electrode diffusion. The maximum value of the current due to the formation of the new phase, and therefore, the number and size of nuclei on the surface, increases as the deposition potential becomes more negative. For PA solutions at pH 0.3, the j_{max} values are practically the same as those obtained in the absence of additive for the same potential step (Figs. 2 and 3). However, at −0.5 V, current of the transient is higher with PA in the solution. In this case, another reaction could be taking place simultaneously, such as the electroreduction of protons from dissociation of the $\boldsymbol{H_2Pic^+}$ and ***HPic*** species or the pyridine–carboxylic acid reduction [21]. At pH 3.0 and 6.5, the values of j_{max} at every deposition potential are lower when the additive is in the solution (Figs. 2a and 3a). This effect is related to the formation of the $[\boldsymbol{Ag}(\boldsymbol{L})^+]$ complexes at the electrode/solution interface in addition to adsorption of ***L*** on the surface of the growing crystals, being the number of active sites available for nucleation, greatly diminished. Diffusion coefficients in the presence of 0.5 mM PA were also estimated by examining the decay of the current at long times using the Cottrell relation. At pH 0.3, 3.0 and 6.5, the values were $D^{0.3(PA)} = 2.5 \times 10^{-5}$ cm^2 s^{-1}, $D^{3.0(PA)} = 1.6 \times 10^{-5}$ cm^2 s^{-1} and $D^{6.5(PA)} = 1.6 \times 10^{-5}$ cm^2 s^{-1}, respectively. The slight diminution of D values in relation to the coefficients determined in the absence of PA at pH 3.0 and 6.5, could also be related to the additive complexating effect.

Comparison of the non-dimensional plots at the same pH and deposition potential suggests that the nucleation mechanism is mainly intermediate in solutions with PA but predominantly instantaneous in its absence. These results indicate that the nucleation rate is lower in solutions containing the additive (Figs. 2b and 3b). It is important to note that this inhibition effect of silver deposition by the additive is clearly observed on the potentiodynamic profiles (Section 3.2).

It was also found that increasing the concentration of PA (results not shown) leads to even more significant changes in the mechanism of silver nucleation observed at pH 3.0 and 6.5. At pH 3.0, the nucleation mechanism is intermediate at any deposition potential, whereas at pH 6.5, progressive nucleation occurs at low overpotentials, with a tendency towards an intermediate to instantaneous mechanism at more negative potentials.

In summary, results obtained from chronoamperometric experiments indicate that, in the absence of additive, the overall mechanism of nucleation changes from intermediate to instantaneous with decreasing pH, across the entire range of applied potential. In the presence of PA at pH 0.3, the mechanism does not vary greatly with the concentration of PA and shows a similar trend to that obtained without additive. This behavior can be expected if the protonated species $\boldsymbol{H_2Pic^+}$ does not form complexes with Ag^+ ions, which are then not adsorbed onto the surface of HOPG, as it was discussed in Section 3.2.

The Ag^+ ions and $[\boldsymbol{Ag}(\boldsymbol{Pic})]$ complexes are the predominant electroactive species in the electrolyte at pH 3.0 and 6.5, respectively (Section 3.1). In addition, adsorption of the ligands is feasible on both, the surface of HOPG and the silver crystallites, modifying the mechanism of silver nucleation and growth.

In the presence of the additive, the normalized current transients (experimental results) lie between those for instantaneous and progressive nucleation (Fig. 3b) and, hence, it is not possible to fit these curves to any of the two limiting situations. The number density of active sites on the surface, N_0, and the nucleation rate constant per active site, A were estimated by nonlinear fitting of every current transient, using the general Eq. (7) [42].

$$j(t) = \left(\frac{zFD^{1/2}c}{\pi^{1/2}t^{1/2}}\right)\left(1-\exp\left\{-N_0\pi kD\left[t-\frac{(1-\exp(-At))}{A}\right]\right\}\right) \quad (7)$$

where $zF = 96485$ C mol^{-1}, the concentration of metal ion is $c = 1.0 \times 10^{-6}$ mol cm^{-3}, the material constant for silver is $k = \left(\frac{8\pi cM}{\rho}\right)^{1/2}$, $M = 107.87$ g mol^{-1} is the molecular mass, and $\rho = 10.5$ g cm^{-3} is the density of silver. In fitting the curves, diffusion coefficients calculated by Cottrell relation were employed.

Figs. 4 and 5 show the dependence of the kinetic parameters calculated by Eq. (7), on the pulse potential, the additive concentration, and the pH of the solution. In Fig. 4, the number of active sites on the substrate, N_0 increases with the overpotential at different pH [5]. It is well known that the nucleation of silver on a foreign substrate mainly begins on the surface defects [43] and, in acid solutions, only a small number of nucleation sites are active (on the surface defects), in the case of an instantaneous nucleation mechanism. However, at higher pH, a greater N_0 with a broad diversity of active sites on the surface have been determined [44], and this feature can be related to the modification of the nucleation mechanism towards a progressive behavior. The increased availability of nucleation sites at pH 6.5 could be due to the presence of functional groups on the HOPG defects as various authors have informed [45,46]. In contrast, the effect of increasing the nucleation rate constant A (Fig. 5), observed at more negative potentials, is directly associated with the nucleation process changing towards an instantaneous mechanism [40]. At pH 0.3, although the number of nucleation sites practically does not change with the additive concentration, the nucleation constant A does decreases significantly. This effect can be explained by assuming that a small amount of zwitterion ***HPic*** is present in solution (ca. 15% of the total PA concentration), with its eventual adsorption on the growing crystallites resulting in an inhibition of the deposition rate. A comparison of Fig. 4a–c, reveals that, at a given potential, N_0 increases with pH, as established from the results of Fig. 3, whereas Fig. 5 shows that the rate constant A

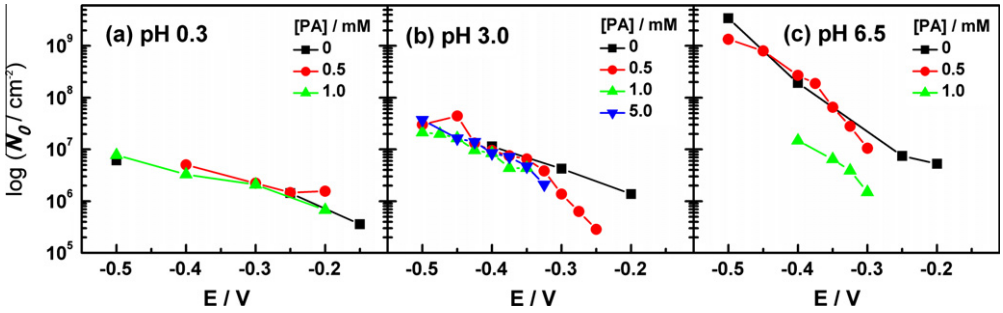

Fig. 4. Dependence of the number density of active sites N_0 on the silver deposition potential onto HOPG electrodes in 1.0 mM $AgClO_4$ + x mM PA ($0 \leqslant x \leqslant 5.0$) and 0.5 M $HClO_4$ pH 0.3 (a) or 0.1 M $KClO_4$ pH 3.0 (b) and pH 6.5 (c).

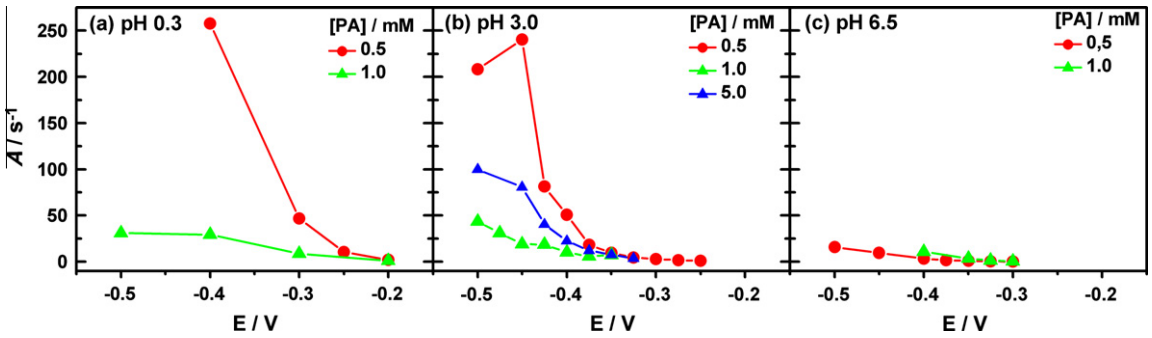

Fig. 5. Dependence of the nucleation rate A on the silver deposition potential onto HOPG electrodes in solutions of 1.0 mM $AgClO_4$ + x mM PA ($0.5 \leqslant x \leqslant 5.0$) and 0.5 M $HClO_4$ pH 0.3 (a) or 0.1 M $KClO_4$ pH 3.0 (b) and pH 6.5 (c).

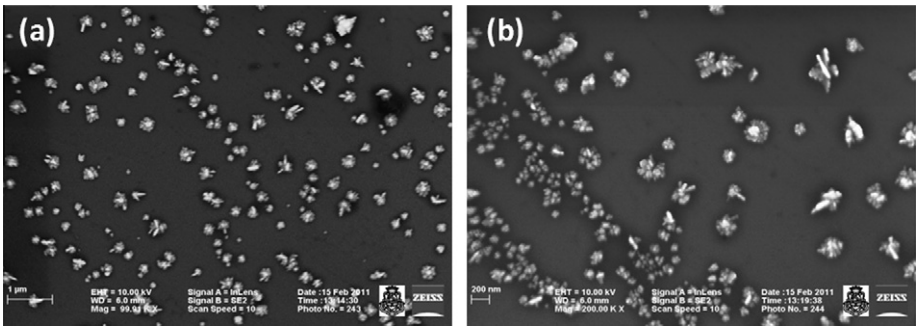

Fig. 6. SEM images of silver nanoparticles electrodeposited on HOPG from 1.0 mM $AgClO_4$ + 0.5 mM PA in 0.1 M $KClO_4$ (pH 3.0) until a charge of -8.5 mC cm^{-2} has been passed at -0.5 V. (a and b) are the same image with different magnification.

decreases as the pH becomes more alkaline, thereby indicating that the nucleation mechanism resembles at a more progressive behavior.

3.4. Morphology of the silver crystallites

SEM images in Fig. 6 shows the silver electrodeposited crystallites onto HOPG, after a pulse of -0.5 V during 45 s in solution containing 0.5 mM PA (pH 3.0). Crystallites formed under these conditions look like small stars, distributed over the whole surface, with no ordered pattern. The image shows 3D silver structures on the surface of HOPG, without formation of a two-dimensional coating. These results confirm a 3-D type of crystal growth on the graphite surface following a Volmer–Weber mechanism [19]. Moreover, even though the mechanism of nucleation is instantaneous at -0.5 V (see Fig. 3b), a large particle size polydispersity is observed in Fig. 6.

In the first stages of growth, three-dimensional clusters are so small that practically there is no noticeable size dispersion of the particles. However, when the size of the crystallites increases with the time of deposition, the polidispersity in particles size is noticeable, regardless of the nucleation mechanism. In order to attain control of the particle size distribution, it is necessary to separate the nucleation and growth steps. Some authors have proposed the application of complex programs of potential pulses in order to eliminate the coupling of depletion layers of adjacent particles with a random spatial distribution on the electrode surface [47,48,10]. The double pulse program includes a first step of nucleation at a large overpotential E_n applied during 5–10 ms and a second pulse of growing at E_g potential, which must be low enough to inhibit formation of new nuclei. During the stage of nucleation, the seeding of nuclei on the HOPG surface is performed. In the second step, the nuclei are grown very slowly. Appropriate E_n and E_g values are selected from the potential

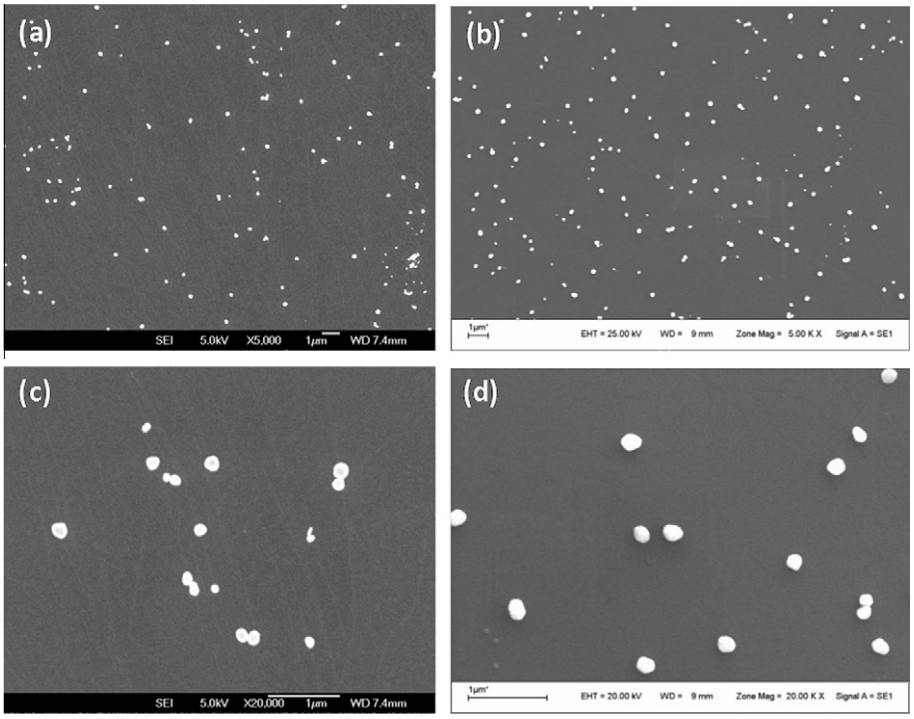

Fig. 7. SEM images of silver nanoparticles electrodeposited on HOPG from 1.0 mM $AgClO_4$ in 0.1 M $KClO_4$ (pH 3.0) after application of a double pulse: $E_n = -0.7$ V, $E_g = -0.05$ V; $t_g = 15$ s, (a) $t_n = 10$ ms, (b) $t_n = 30$ ms and $E_n = -0.7$ V, $t_n = 10$ ms; $t_g = 15$ s, (c) $E_g = -0.05$ V, and (d) $E_g = -0.07$ V.

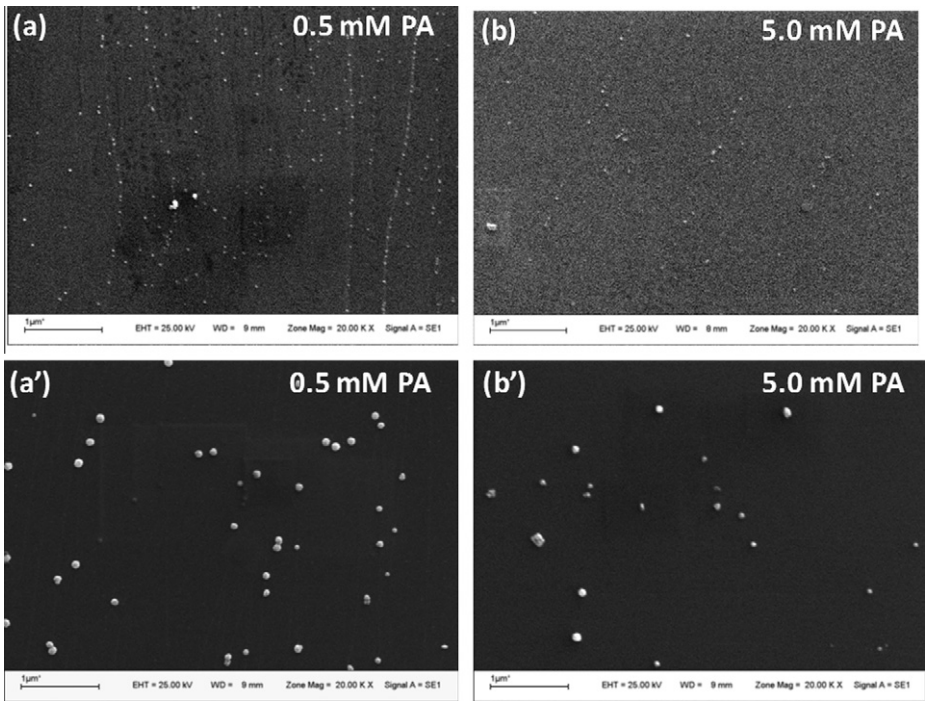

Fig. 8. SEM images of silver nanoparticles electrodeposited on HOPG from 1.0 mM $AgClO_4$ and x mM PA solutions in 0.1 M $KClO_4$ (pH 3.0), where $x = 0.5$ (a and a′) or $x = 5.0$ (b and b′). Double potential pulse parameters: $E_n = -0.85$ V; $E_g = -0.05$ V (a and b) or -0.15 V (a′ and b′); $t_n = 10$ ms and $t_g = 300$ s.

colored zones in the j/E potentiodynamic profiles of Fig. S1 in the Supporting information.

Figs. 7–9 show SEM images of silver crystallites deposited onto HOPG in the absence and presence of PA at various pH, by applying a double pulse program. When silver is deposited in the absence of PA at pH 3.0, the increase of the time for nucleation at $E_n = -0.7$ V produces an increase on the nuclei density and the spherical silver particles maintain their dimensions (Fig. 7a and b). Moreover, when E_g is more negative, the amount of particles is approximately the same but their diameter is slightly increased (Fig. 7c and d). Similar effects were found in the presence of the additive, for a selected value of E_n that was more negative than that applied in the

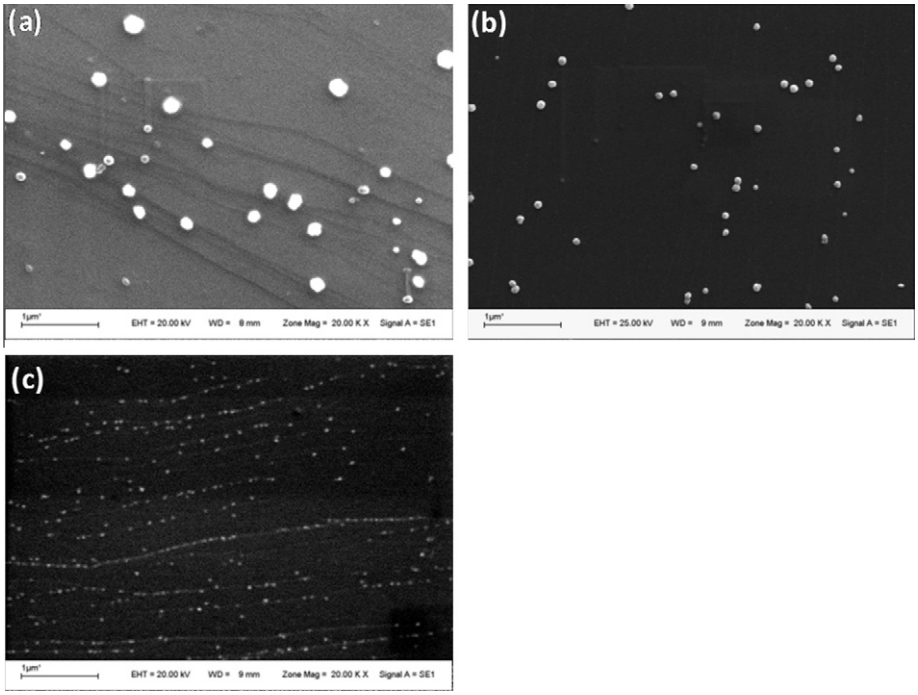

Fig. 9. SEM images of silver nanoparticles electrodeposited on HOPG from 1.0 mM $AgClO_4$ and 0.5 mM PA solutions at pH of 0.3 (a); 3.0 (b) and 6.5 (c). Double potential pulse parameters: $E_n = -0.7$ V (a) or $E_n = -0.85$ V (b and c); $E_g = -0.08$ V (a) or $E_g = -0.15$ V (b and c); $t_n = 10$ ms and $t_g = 15$ s.

additive absence, as a consequence of the deposition peak in the potentiodynamic profiles (Fig. 1b and c) being displaced in 150 mV towards more cathodic regimes. Significant influence on the particle size in the presence of PA was also observed upon increasing growth overpotential. In Fig. 8a and a′ the mean particle diameter is around 30 nm at $E_g = -0.05$ V, but falls between 70 and 100 nm at $E_g = -0.15$ V. Moreover, as observed in the potentiodynamic experiments, a greater inhibition of the electrodeposition process (lower density of crytallites) results from increasing the PA concentration in solution (Fig. 8b and b′).

Comparison of Figs. 6 and 9b reveals that even though both silver deposits were obtained with 0.5 mM PA solutions at pH 3.0, the morphology of the structures is very different. Star-like crystallites with a large dispersion of sizes were deposited with a simple pulse potential, while the application of a double potential pulse produced spherical silver particles that kept shape after 5 min of growing (data not shown). In the single step case, the potential is sufficiently negative to allow for the occurrence of simultaneous nucleation and growth of the particles throughout the duration of the pulse and, certainly, both processes can occur on the growing nuclei and the HOPG surface. There is no doubt that this effect leads to the formation of large structures, with some asymmetry and variation in their mean size. By contrast, in the double pulse potential case (Fig. 9), the particle density on the surface is determined by the duration and potential of the nucleation step. For this reason, during the growth step, there is no formation of new nuclei and the particles increase the size continuously.

In this work, silver was deposited onto HOPG from solutions containing PA at various pH. Fig. 9 shows images of the particles obtained by a double pulse program as the chemical identity of the predominant PA species in solution varies. At pH 0.3 (Fig. 9a), silver particles are randomly deposited over the whole surface with a large polydispersity in size, as in the absence of PA (Fig. 7d). Upon increasing the solution pH to 3.0, ***HPic*** becomes the principal PA chemical species, and the particles are spherical and smaller (between 70 and 100 nm) than in the previous case (Fig. 9b). However, the presence of $\boldsymbol{Pic}^-$ species at pH 6.5 leads to a remarkable size reduction and increase in the density of nuclei, which are preferentially deposited on the HOPG defects. SEM images in Fig. 9 are consistent with the variation of N_0 values as the solution pH changes (Fig. 4).

The fact that the decrease of crystallite growth rate becomes more remarkable at higher the solution pH, is due to increasingly strong adsorption of additive molecules on the silver structures resulting in smaller and spherical nanoparticles. Moreover, the increase of pH also leads to the activation of sites on the HOPG surface, thereby causing an increase in the number of active sites N_0.

4. Conclusions

The nucleation and growth processes of silver crystallites onto HOPG electrodes in the presence of PA have been studied using cyclic voltammetry and chronoamperometry. The potentiodynamic experiments have shown that the onset potential for silver electrodeposition is shifted with an increase in solution pH, resulting in a noticeable inhibition effect on both silver electrodeposition and dissolution processes. Effects such as adsorption of the additive species and formation of complexes in the solution can be controlled by changing the analytical concentration of PA and pH of the solution. The chronoamperometric results have shown that the first steps of silver deposition proceed by a 3D diffusion-controlled growth and that the mechanism depends upon the chemical nature of the electroactive species in the electrolyte.

At pH 0.3, protonated $\boldsymbol{H_2Pic}^+$ is the relevant species in solution, and the potentiodynamic behavior of silver deposition on HOPG is practically not modified. The nucleation and growth mechanism is predominantly instantaneous and silver nanostructures are deposited directly by electroreduction of Ag^+ ions, with the amount of $[\boldsymbol{Ag}(\boldsymbol{HPic})^+]$ species being negligible.

At pH 3.0, the solution composition includes $\boldsymbol{Ag}^+$, $[\boldsymbol{Ag}(\boldsymbol{HPic})^+]$, and ***HPic*** species. At 0.5 mM PA, the electroreduction of free-Ag^+ ions is the main reaction, due to the negligible concentration of $[\boldsymbol{Ag}(\boldsymbol{HPic})^+]$. Evidence of electron transfer inhibition is attained

from adsorption of the zwitterion species (diminution of the number density of active sites). In this case, the nucleation mechanism changes from intermediate to instantaneous as the deposition potential becomes more negative.

In contrast at pH 6.5, the predominant chemical entity is the anion ***Pic***$^-$, and the rate of mass transfer is diminished by complexation and adsorption processes dependent on the deposition potential [29]. Under these conditions, a significant shift towards progressive nucleation with 3D diffusion-controlled growth is found for silver electrocrystallization. The nucleation sites density N_0 is increased and the nucleation rate constant A is strongly diminished at every potential. SEM images recorded after application of single or double potential pulses show differences in surface distribution, and size and geometry of the silver nanostructures.

Acknowledgements

The authors gratefully acknowledge the financial support from CONICET, FONCyT and SECyT-UNC. C.I.V. thanks also CONICET for the fellowships granted. Authors also gratefully acknowledge to Dr. Marcia L. Temperini and Dr. Gustavo Andrade for acquiring the scanning electron micrographs (San Pablo University, Brazil) and Dr. A. Granados for the useful help of the NMR analysis (INFIQC, Facultad Ciencias Químicas, UNC).

Appendix A. Supplementary material

Supplementary data associated with this article can be found, in the online version, at http://dx.doi.org/10.1016/j.jelechem.2012.12.017.

References

[1] A. Dolati, A. Afshar, H. Ghasemi, Mater. Chem. Phys. 94 (2005) 23.
[2] G.M. Zarkadas, A. Stergiou, G. Papanastasiou, Electrochim. Acta 50 (2005) 5022.
[3] H. Natter, R. Hempelmann, J. Phys. Chem. 100 (1996) 19525.
[4] B.H.R. Suryanto, Ch.A. Gunawan, X. Lu, Ch. Zhao, Electrochim. Acta 81 (2012) 98.
[5] D. Grujicic, B. Pesic, Electrochim. Acta 47 (2002) 2901.
[6] A. Hubin, D. Gonnissen, W. Simons, J. Vereecken, J. Electroanal. Chem. 600 (2007) 142.
[7] W. Li, G.S. Hsiao, D. Harris, R.M. Nyffenegger, J.A. Virtanen, R.M. Penner, J. Phys. Chem. 100 (1996) 20103.
[8] S.R. Nambiar, P.K. Aneesh, Ch. Sukumar, T.P. Rao, Nanoscale 4 (2012) 4130.
[9] L. Guo, A. Thompson, P.C. Searson, Electrochim. Acta 55 (2010) 8416.
[10] R.M. Penner, J. Phys. Chem. B 106 (2002) 3339.
[11] R.M. Nyffenegger, R.M. Penner, Chem. Rev. 97 (1997) 1195.
[12] T. Dobrovolska, R. Kowalik, P. Zabinski, I. Krastev, Bulg. Chem. Commun. 40 (2008) 254.
[13] E. Budevski, G. Staikov, W.J. Lorenz, in: Electrochemical Phase Formation and Growth, VCH, Weinheim, 1996.
[14] D. Grujicic, B. Pesic, Electrochim. Acta 50 (2005) 4426.
[15] P.F.J. de Leon, E.V. Albano, R.C. Salvarezza, Phys. Rev. E 66 (2002) 0426011.
[16] Zh. Lin, Bu. Xie, J. Chen, J. Sun, G. Chen, J. Electroanal. Chem. 633 (2009) 207.
[17] K. Márquez, G. Staikov, J.W. Schultze, Electrochim. Acta 48 (2003) 875.
[18] C. Ramírez, E.M. Arce, M. Romero-Romo, M. Palomar-Pardavé, Solid State Ion. 169 (2004) 81.
[19] L.L. Wang, X.C. Ma, Y. Qi, P. Jiang, J.F. Jia, Q.K. Xue, J. Jiao, X.H. Bao, Ultramicroscopy 105 (2005) 1.
[20] A.L. Portela, G.I. Lacconi, M. López Teijelo, J. Electroanal. Chem. 495 (2001) 169.
[21] A.L. Portela, M. López Teijelo, G.I. Lacconi, Electrochim. Acta 51 (2006) 3261.
[22] J. Barthelmes, W. Plieth, Electrochim. Acta 40 (1995) 2487.
[23] R.T. Pötzschke, C.A. Gervasi, S. Vinzelberg, G. Staikov, W.J. Lorenz, Electrochim. Acta 40 (1995) 1469.
[24] K.H. Ng, H. Liu, R.M. Penner, Langmuir 16 (2000) 4016.
[25] S. Kotrlý, L. Šucha, Handbook of chemical equilibria in analytical chemistry, in: Ellis Horwood Series in Analytical Chemistry, Chichester, England, 1985.
[26] W. Lewandowski, M. Kalinowska, H. Lewandowska, J. Inorg. Biochem. 99 (2005) 1407.
[27] M. Kalinowska, M. Borawska, R. Swisłocka, J. Piekut, W. Lewandowski, J. Mol. Struct. 834–836 (2007) 419.
[28] N.L. Brennan, Ch.L. Barnes, E. Bosch, Inorg. Chim. Acta 363 (2010) 3987.
[29] C.I. Vázquez, Electrochemical formation of metallic and bimetallic nanostructures, influence of the organic compounds, Ph.D. Thesis, Córdoba, Argentina, 2012.
[30] N. Hernández, J.M. Ortega, M. Choy, R. Ortiz, J. Electroanal. Chem. 515 (2001) 123.
[31] B.E. Breyfogle, C.J. Hung, M.G. Shumsky, J.A. Switzer, J. Electrochem. Soc. 143 (1996) 2741.
[32] S.G. García, D.R. Salinas, C. Mayer, J.R. Vilche, H.J. Pauling, S. Vinzelberg, G. Staikov, W.J. Lorenz, Surf. Sci. 316 (1994) 143.
[33] B. Bozzini, C. Mele, L. D'Urzo, V. Romanello, J. Appl. Electrochem. 36 (2006) 973.
[34] G. Lu, G. Zangari, J. Phys. Chem. B 109 (2005) 7998.
[35] A.E. Alvarez, D.R. Salinas, J. Electroanal. Chem. 566 (2004) 393.
[36] A.R. Alonso, G.T. Lapidus, I. González, Hydrometallurgy 85 (2007) 144.
[37] G. Gunawardena, G. Hills, I.J. Montenegro, B.R. Scharifker, J. Electroanal. Chem. 138 (1982) 225.
[38] B.R. Scharifker, G. Hills, Electrochim. Acta 28 (1983) 879.
[39] A.J. Bard, L.R. Faulkner, Electrochemical methods, in: Fundamentals and Applications, second ed., John Wiley & Sons, Inc., New York, 2001.
[40] M. Palomar-Pardavé, I. González, N. Batina, J. Phys. Chem. B 104 (2000) 3545.
[41] G. Gunawardena, G. Hills, I.J. Montenegro, J. Electroanal. Chem. 138 (1982) 241.
[42] B.R. Scharifker, J. Mostany, J. Electroanal. Chem. 177 (1984) 13.
[43] E.C. Walter, B.J. Murray, F. Favier, G. Kaltenpoth, M. Grunze, R.M. Penner, J. Phys. Chem. B 106 (2002) 11407.
[44] M.H. Hölzle, C.W. Apsel, T. Will, D.M. Kolb, J. Electrochem. Soc. 142 (1995) 3741.
[45] M.R. Deakin, K.J. Stutts, R.M. Wightman, J. Electroanal. Chem. Interf. Electrochem. 182 (1985) 113.
[46] R.L. McCreery, Chem. Rev. 108 (2008) 2646.
[47] G. Sandmann, H. Dietz, W. Plieth, J. Electroanal. Chem. 491 (2000) 78.
[48] H. Liu, F. Favier, K. Ng, M.P. Zach, R.M. Penner, Electrochim. Acta 47 (2001) 671.